Received: 20 July 2021 | Revised: 15 November 2021 | Accepted: 8 December 2021

DOI: 10.1002/app.52052

ARTICLE

Applied Polymer SCIENCE WILEY

Sintering graded foamed beads: Compressive properties

Fabrizio Errichiello[1,2] | **Aniello Cammarano**[1] | **Ernesto Di Maio**[2,3] | **Luigi Nicolais**[1,3]

[1]Materias S.r.l., Naples, Italy

[2]Foamlab, University of Naples Federico II, Naples, Italy

[3]Dipartimento di Ingegneria Chimica, dei Materiali e della Produzione Industriale, University of Naples Federico II, Naples, Italy

Correspondence
Ernesto Di Maio, foamlab, University of Naples Federico II, Piazzale Vincenzo Tecchio, 80, 80126, Naples, NA, Italy.
Email: edimaio@unina.it

Abstract

Designing the foam structures in terms of density and morphology gives the chance to tune their mechanical and functional properties to the specific application. Nowadays, this design has been leveled up by the introduction of graded foams which are characterized by spatially nonuniform densities and/or morphologies. Graded foams have proved superior compared to uniform one in numerous examples and loading conditions but in pure compressive loading, where properties such as the Young's modulus of graded foams are always inferior to uniform ones. When using sintered beads foams, macroscopic pure compression may induce local bending on the single bead, which can be exploited to induce stiffening. This thesis was investigated on both polystyrene and thermoplastic polyurethane samples made by foamed beads sintered in a cylindrical mold. The response to compressive tests of graded foams made by sintering beads having nonuniform cells structures was compared to the uniform counterparts. The results evidenced that, at same average density, foams had up to a 30% ca. of increase of the Young's modulus when the beads are characterized by a denser outer layer.

KEYWORDS

compressive properties, foams, graded, PS, sintered, TPU

1 | INTRODUCTION

In the modern continuous research for better materials, biomimicry has always been a valued choice as the wonderful natural materials that are very often strong, tough, and lightweight serve as a source of inspiration for every materials designer.[1,2] Animal's bones, tree trunks and carapaces, among others, are all porous, with a nonuniform spatial distribution of size, number, orientation, or shape of the pores. Through hundreds of millions of years of evolution, (multi)-graded porous materials have been Nature's way to boost mechanical and functional performances or, said differently, to optimize the use of the matter.[1]

Nowadays, graded foams (metallic,[3–5] ceramic,[6,7] and polymeric[8,9]) are gaining interest and several strategies are reported to achieve foams with graded densities and/or morphologies, along with theoretical studies[10,11] which point to enhanced properties of the graded foams with respect to their uniform counterparts.[12–16] Property improvement has been observed in impact and static flexural loading.[10,17–19] For instance, Uddin and coworkers proved that significant improvement in strength and energy absorption performance can be achieved through density gradation of polyurea foams in footwear design.[17] Polit and coworkers investigated the static bending and buckling response of nanocomposites foams, showing that the design of the localized additive loading and of porosity (both in symmetric and asymmetric configuration) can significantly affect mechanical performance.[18] Kazemi utilized a uniform as well as layered polyurethane foams in sandwich structures showing that the arrangement of the layers induced a 7-fold increase of energy absorption capacity of a layered foam with respect to a uniform foam with equal average density.[19] Cui et al. provided an analytical

model of the behavior of convex-density-graded as well as concave-density-graded foams in helmets application and illustrated via a numerical testing the advantages of the gradient density function design in energy absorption.[10]

Among the properties of interest of porous solids, the response to compressive loads is particularly important in view of the typical foam application fields.[4,10] Young's modulus, together with collapse plateau stress and densification deformation,[20–22] is used to quantify the foam response in compressive mode. Although graded foams often outperform uniform ones, it is easy to prove that a graded/layered one always has a Young's modulus smaller than a uniform foam with same average density, in case the density layering is parallel to the compression load (in iso-stress loading mode, see the proof in Appendix A). Thus, graded foams are not recommended when the aim of foam-structure design is the increase of the stiffness in pure compression loading. It is conversely well known that in bending loading layered systems where elements with larger Young's modulus are brought far from the neutral axis are stiffer than their uniform counterpart.

In polymer technology, bead foaming or steam chest molding is a common technology to mass-produce foamed parts with complex shapes. It is a two-step method, where first pre-expanded beads (mm-size, spherical foamed polymeric particles) are formed, and then the beads are introduced in a mold. Here a temperature rise induces polymer softening and a further (relatively small) expansion, which induce beads sintering to form a monolith.[23,24] In the final foamed monolith, the earlier presence of the separate beads is observable by naked eye and the structure can be described as dual scale: (i) the mm-sized beads and (ii) the micron-sized cells within the beads (see Figure 1a,b). Often, the beads boundary/intersection (also addressed to as interbeads layer) is a relatively thick wall with different (often negligible) porosity in relation to the beads core (see Figure 1c).

It has been observed that the interbeads layer may affect the foam properties to an extent that depends on the relative size of the core and interbeads layer, their density and the interbeads bonding.[24] Moreover, the latter describes the quality of the adhesion between two beads and is due to the polymer self-diffusion and it requires high enough temperature and contact time. Perfect interbeads bonding requires the memory loss of chain configuration and is classically described in terms of chain relaxation time, or reptation time, τ_{rep}.[25] A representative longest relaxation time can be evaluated with the intersect frequency at which dynamic moduli G' and G'' intersect in mechanical spectroscopy (τ_i). Values of τ_i ~10^{-1} to 10^{1} s have been measured depending on the polymer and the temperature[26] which may result compatible to achieve sufficient interbeads bonding within the bead foaming process timing. For instance, in pure compression loading, it has been observed that the meso-scale morphology of the bead boundaries (as the one observed in Figure 1b) is locally subjected to multi-axial loading.[21,27–29] The complex mechanical behavior governed by the morphological features (at the dual scale) of the foam and the physical properties of the polymer (i.e., crystallinity and orientation) can be exploited by applying the graded foaming technology to bead foaming. Specifically, the foamed structure of the single bead can be designed to fine tune the local response and improve performances in pure macroscopic compression loading. In this work, a recently introduced technology,[8] based on nontrivial sorption stage of the blowing agent (BA) prior to foaming, was adopted to produce graded foamed beads. The beads are then allowed to sinter in cylindrical samples and tested in compression to study the effect of the graded morphology on the mechanical performance.

2 | MATERIALS AND METHODS

Thermoplastic polyurethane (TPU), code 3080au, was provided by Great Eastern Resins Industrial Co., Ltd. (GRECO, Taichung City, Taiwan). The polymer, in the form of ellipsoidal granules with a size of 3 × 2 mm ca., is characterized by an average molecular weight of

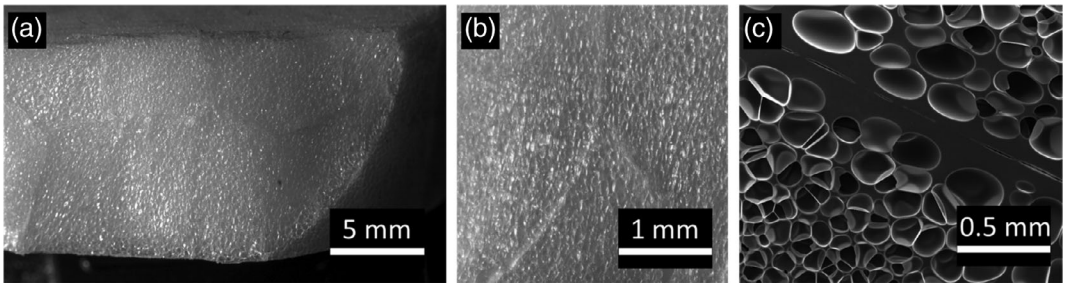

FIGURE 1 Bead foams morphology at different scales: (a) optical image of a section of a cylindrical sample; (b) optical image of the intersection among three beads; (c) scanning electron image of the intersection of two beads

500 kDa and a density of 1.14 g/cm^3. Polystyrene (PS), code N2380, was provided by Versalis SpA (Mantua, Italy). The polymer, in the form of spherical granules with a size of 3 mm ca., is characterized by an average molecular weight, density and melt flow index of 300 kDa, 1.05 g/cm^3 and 2.0 g/10 min at 200°C and 10 kg, respectively. The BAs, He, CO_2, N_2, and a N_2/CO_2 mixture (80/20 v/v), were supplied by SOL S.p.A. (Monza, Italy).

The batch foaming equipment used to prepare the foamed samples is a 0.3L custom-made thermo-regulated pressure vessel (model BC-1, High Pressure Equipment Co., Erie, PA, USA), detailly described elsewhere.[30] For the temperature control, an electrical heater controlled by a PID thermoregulator (mod. 1850, Gefran S.p.A., Provaglio d'Iseo [BS], Italy) which reads the temperature inside the vessel by using a Pt100 and the temperature of the heating jacket by a J-thermocouple. A pressure transducer (TK, Gefran S.p.A., Provaglio d'Iseo [BS], Italy) was used to measure pressures during saturation step and to register pressure histories during blowing agent discharge. The pressure discharge system consists of a discharge ball valve (model 15-71 NFB, High Pressure Equipment Co., Erie, PA, USA), an electromechanical actuator (model 15-72 NFB TSR8, High Pressure Equipment Co., Erie, PA, USA) and an electrovalve. Two volumetric pumps (mod. 500D, Teledyne ISCO, Lincoln, NE, USA) were utilized to control the pressure history of the BAs during sorption.

To achieve foamed samples with a pre-defined density, a fixed mass (0.95 and 0.425 g, respectively, for achieving 200 and 100 kg/m^3 final foam density) of polymer granules is placed inside a cylindrical steel mold with a diameter of 25 mm and a height of 9 mm. The mold is placed into the pressure vessel, which was then closed and brought to a temperature of 140°C for TPU and 110°C for PS. Timing for bringing the pressure vessel to the desired temperature was 20 and 15 min, respectively, with ca. 2°C overshoot. Subsequently, the system has been subjected to the BA sorption step according to the specific test conditions (see Table 1), designed to achieve uniform as well as graded structure (in terms of density as well as morphology). The time dependent sorption step is attained by the serial interface of the ISCO pump controller. After the sorption, temperature control was turned off and foaming occurred by venting the pressure vessel through the discharge ball valve, at a fixed pressure release rate of 100 MPa/s. At foaming, the granules become foamed beads which may eventually sinter together to form a monolith, if processing conditions are adequate. It is worth noting, here, that this "one step" sintering method is different from the two-step method reported in the scientific and technical literature of the bead foaming technology. Pressure vessel opening for retrieving the foamed samples took ca. 2 min, during which the samples were exposed to decreasing, noncontrolled temperatures.

Final foam density was measured according to ASTM-D1622-03. Foam morphologies were observed by scanning electron microscope (SEM) (LEICA S440) at an accelerating voltage of 20 kV, at various magnifications.

Uniaxial compression tests were performed using the METRAVIB DMA +1000 (ACOEM) with cylindrical plate configuration. Each sample was subjected to compression with a displacement rate of 0.3 mm/min up to 50% deformation. In this context, the Young's Modulus was chosen as the benchmark parameter. Tests were performed in three replicates.

Processing conditions to obtain the graded morphologies were selected to design the interbeads layer between foamed beads. Specifically, this study aimed to compare bi-layer foam structures (with a core and an outer foamed layer characterized by different densities and/or morphologies) with same average density uniform foam structures.

TABLE 1 Foaming experiments sorption conditions

Sample	Mass [g] (foam average density [kg/m^3])	Sorption stage 1			Sorption stage 2		
		BA_1	P [bar]	t_{sorp1} [min]	BA_2	P [bar]	t_{sorp2} [min]
TPU1	0.95 (100)	N_2/CO_2	110	90	\	\	\
TPU2	0.95 (100)	N_2/CO_2	140	90	He	150	2
TPU3	0.95 (100)	N_2/CO_2	100	90	He	100	5
TPU4	0.95 (100)	N_2/CO_2	150	90	N_2/CO_2	220	2
PS1	0.95 (100)	CO_2	130	90	\	\	\
PS2	0.95 (100)	CO_2	130	90	CO_2	100	2
PS3	0.425 (50)	CO_2	130	90	\	\	\
PS4	0.425 (50)	CO_2	130	90	CO_2	100	2

Note: Refer to text for variable definition.

2.1 | Design of the sorption stage

The sorption stage was designed in order to form graded foamed beads with an effective layering which should be observable but, most importantly, which should prove effective on mechanical properties. In case of beads having a characteristic size (diameter, L) of ca. 1 mm, the layering was designed at the sub-millimetric scale. In the graded-foaming method proposed by Trofa et al.,[8] a single dimensionless parameter (Π), defined as the ratio between the penetration depth of a pressure change effect (δ) and the sample characteristic dimension (L), suffices to design the process according to the desired layering. Equivalently, δ is the square root of the product of the mutual polymer/BA diffusivity (D) and the sorption time (t_{sorp}) after the pressure change ($\delta = [Dt_{sorp}]^{1/2}$).

It is thus possible to define the timing for the desired BA concentration profile when D is known and δ is set, for example, as equal to 0.1 mm.

Data on mutual diffusivities of the polymer/BA couples can be found in the literature and data interpolation procedure allows estimating the Ds at experimental conditions of interest here (see Appendix B).

The time dependent sorption stage foaming technique is highly versatile and allows a large variety of multilayered foamed structure.[8,31] In this context, some examples of two-layered structures were produced by foaming beads samples after a two-stage sorption program. During the first stage (sorption stage 1), a uniform concentration of the first blowing agent (BA_1) is achieved by keeping the polymer at a constant pressure for a sorption time of the *first* stage, $t_{sorp1} >> L^2/D_1$, (D_1 is the polymer/BA_1 mutual diffusivity). After t_{sorp1}, sorption conditions are abruptly changed (within a swap time, $t_{swap} << L^2/D_1$, in our case $t_{swap} = 5$ s) to the second stage sorption conditions where the system is kept for a t_{sorp2}, required to the first blowing agent to leave the polymer solution within an outer layer of thickness $\delta_1 = [D_1\ t_{sorp2}]^{1/2}$. In the case the second sorption stage is conducted with a BA_2 different from BA_1, t_{sorp2} is also defining the penetration depth of the second blowing agent, $\delta_2 = [D_2\ t_{sorp2}]^{1/2}$ (D_2 the polymer/BA_2 mutual diffusivity). Figure 2 schematizes the possible layer design criterion. In particular, in the case of a BA_2 different from BA_1, Figure 2a clarifies that δ_1 is different than δ_2 due to different diffusivities of the BA_1 and BA_2 in the same polymer and t_{sorp2} can be selected balancing BA_1 impoverishment and BA_2 penetration. When the second sorption stage is conducted without change of the blowing agent nature, there is only a single penetration depth δ_1, both in case of additional sorption due to increased pressure (Figure 2b) and in the case of decreased pressure (Figure 2c).

In terms of partial pressure of the BA (external phase), sorption conditions are listed for the polymers under investigation in Table 1. TPU1, PS1, and PS3 are the control foams with uniform morphology, made of TPU (with a density of 100 kg/m^3) and PS (with a density of 100 and 50 kg/m^3). TPU2 and TPU3 follow the strategy depicted in Figure 2a, where a BA_2 different from BA_1 is utilized. At the end of the sorption stage 1, where a uniform N_2/CO_2 (as BA_1) concentration profile was attained, a purge by He (as BA_2) is conducted. BA_2 is characterized by a much smaller solubility as regards to BA_1 hence is responsible for the achievement of foams with an outer layer δ with a much higher density. Having swapped BA_1 with BA_2 and keeping this condition for t_{sorp2} induces a BA_1 loss from the sample surface within $\delta_1 = (D_1 t_{sorp2})^{1/2}$. As D_1 ~10^{-9} m^2 s^{-1} (see Appendix B), t_{sorp2} ~10^2 s. Concurrently, BA_2 diffuses into the sample within $\delta_2 = (D_2 t_{sorp2})^{1/2}$. Data on He diffusivity in PS and TPU are not available. However, it can be assumed much larger than one of CO_2 and N_2, also in view of

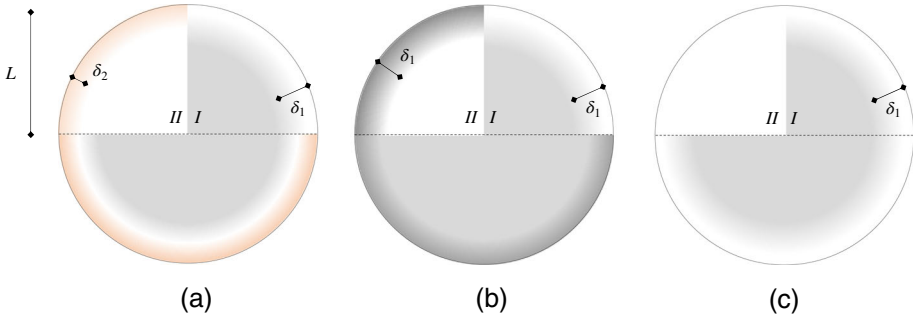

FIGURE 2 Two-layered foam design: I and II quadrant describe, respectively, the BA_1 and the BA_2 concentration profiles at the end of the two-stage sorption, right before the pressure release for foaming; bottom half describes the idealized concentration profile attained at the end of the sorption by the two BAs. (a) $BA_1 \neq BA_2$; (b) $BA_1 = BA_2$, outer layer less dense than core layer, as a consequence of larger BA concentration; (c) $BA_1 = BA_2$, outer layer denser than core layer as a consequence of smaller BA concentration) [Color figure can be viewed at wileyonlinelibrary.com]

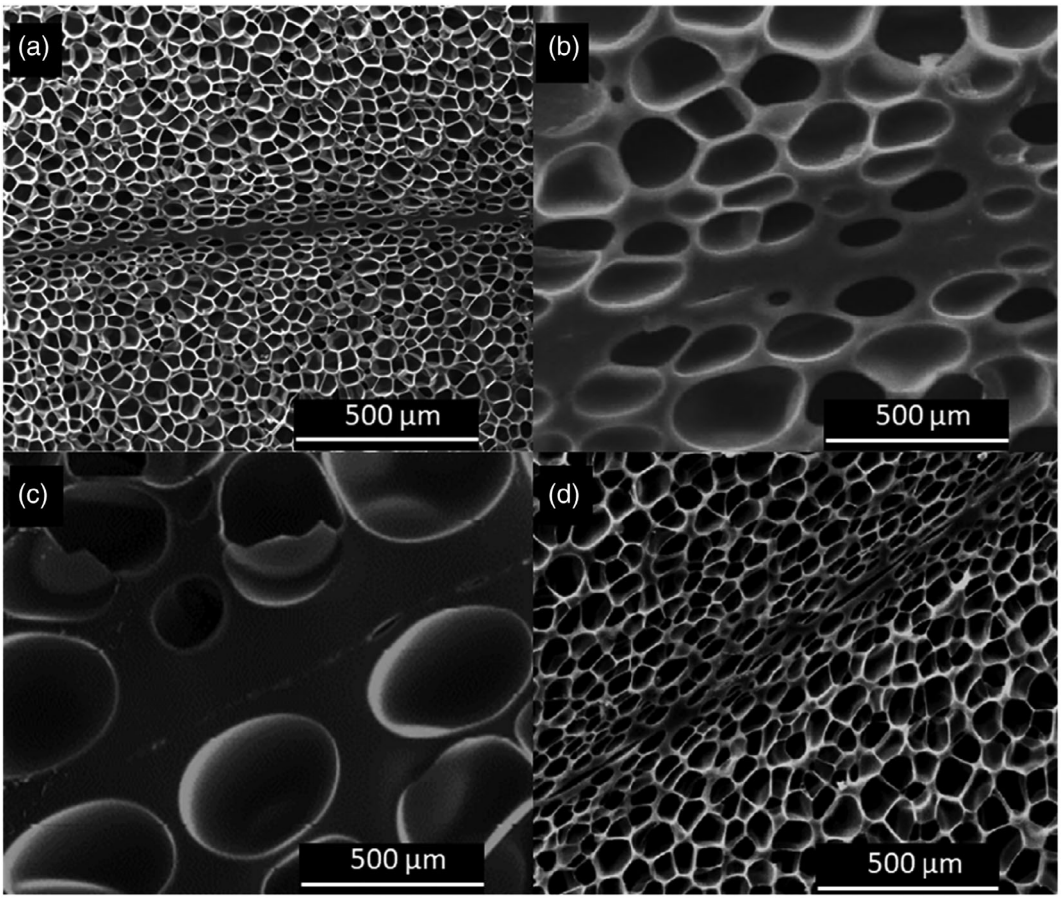

FIGURE 3 Images of foamed TPU samples obtained by SEM: (a) TPU1, (b) TPU2, (c) TPU3, and (d) TPU4

the smaller size of the molecule. Within t_{sorp2}, hence, it is reasonable to assume that $\delta_2 \sim L$. Consequently, as it will be seen in the following, TPU2 and TPU3 are characterized by a denser outer foamed layer. TPU4 follows the strategy depicted in Figure 2b, where sorption stage 2 is conducted at a higher pressure with the same BA (no BA swap). Keeping this condition for t_{sorp2} induces an increase of the BA concentration within $\delta_1 = (D_1 t_{sorp2})^{1/2}$ and a corresponding density decrease. TPU4 is characterized by a denser core and a less dense outer layer. Finally, PS2 and PS4 follow the strategy depicted in Figure 2c. Here, The BA1 pressure is reduced in the second sorption stage, thereby inducing a formation of a denser skin because of the reduced BA concentration corresponding to the lower pressure.

3 | RESULTS AND DISCUSSION

3.1 | Morphologies of the achieved foams

Foam morphology of TPU1 is uniform in terms of pore size and density distribution, as shown in Figure 3a. TPU2, TPU3, and TPU4 are conversely characterized by a graded morphology as shown in Figure 3b–d. In particular, the SEM images of TPU2 and TPU3 show an increasing thickening of the interbeads layer. Thickening is even more pronounced in TPU3, because of the longer t_{sorp2} (5 min) and a corresponding increase of δ_1. The sorption program for sample TPU4 is designed as a counterexample to achieve foams characterized by a less dense interbeads layer due to an increase of the BA pressure in the second sorption stage (see Figure 3d).

Optical microscope images of foamed PS samples with a density of 100 kg/m^3, namely PS1 and PS2 are reported in Figure 4. Similarly to TPU samples, thicker and denser interbeads layers are observable in Figure 4c, d (PS2, graded) as compared to Figure 4a,b (PS1, uniform). Finally, Figure 5 shows images of foamed PS samples with a density of 50 kg/m^3, with similar results.

3.2 | Mechanical properties of the achieved foams

The cylindrical samples obtained by sintering foamed beads of TPU and PS were subject to uniaxial compression tests in order to compare the mechanical properties

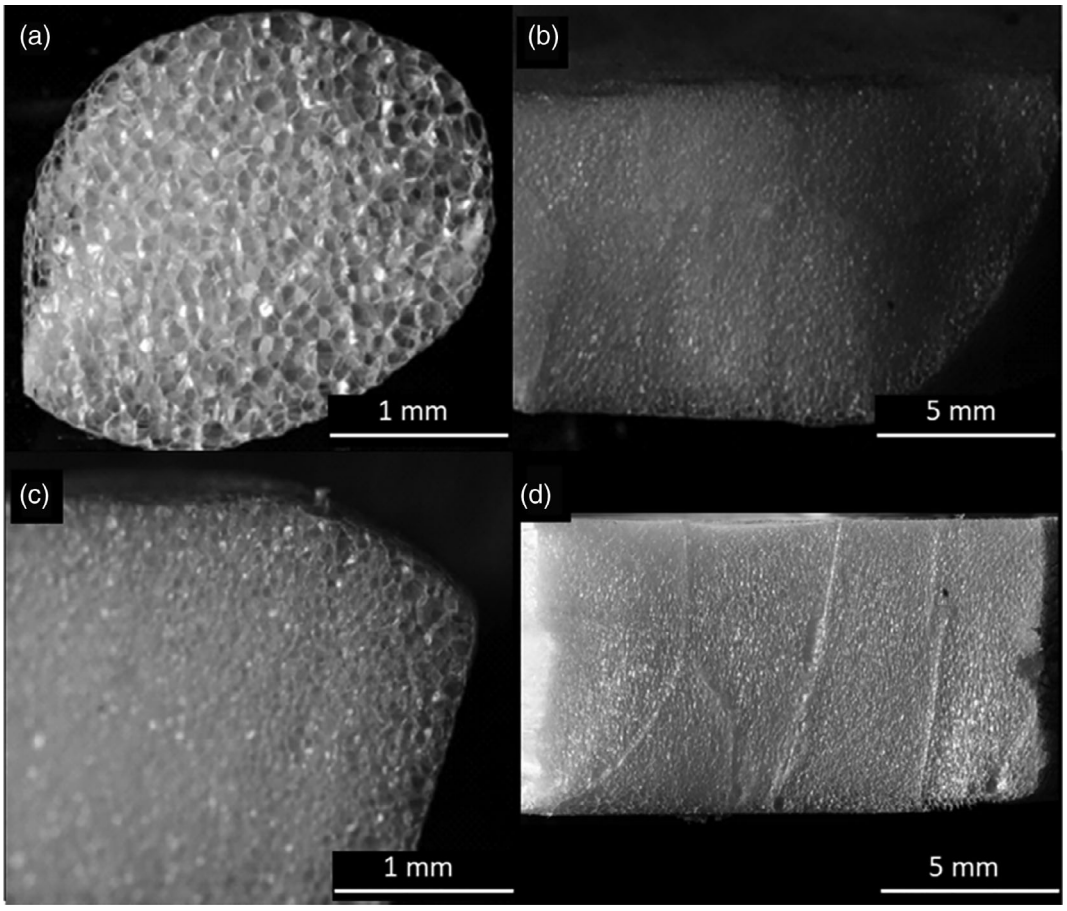

FIGURE 4 Images of foamed PS1 and PS2 samples obtained by optical microscopy at different magnifications: (a) and (b) PS1, (c) and (d) PS2

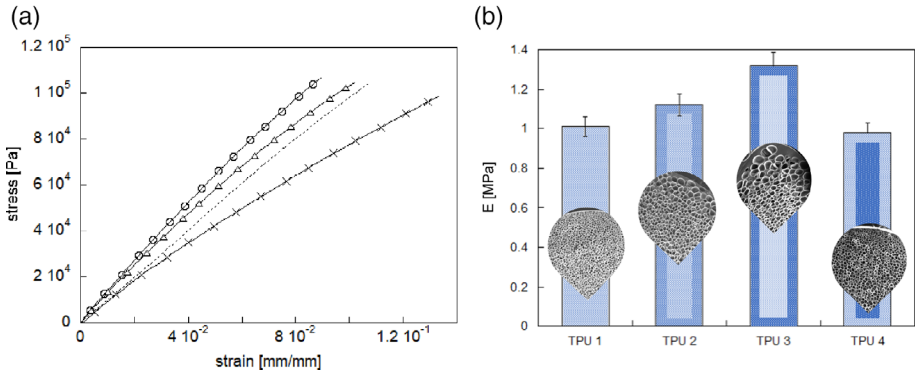

FIGURE 5 (a) Stress–strain curves in uniaxial static compression of the TPU samples: TPU1 (dotted line), TPU2 (△), TPU3 (○) and TPU4 (×); (b) Young's moduli of the different TPU foamed samples, SEM images of the corresponding foamed beads in the insets [Color figure can be viewed at wileyonlinelibrary.com]

of the uniform foams with the ones of the graded foams. Figure 5a illustrates the elastic region of the stress–strain curves, representing the data acquired by the mechanical testing of TPU foamed samples. The values of the Young's Modulus are represented in Figure 5b and reported in Table 2.

As expected, Young's modulus of the graded foamed samples differs from the modulus of the uniform foamed sample (TPU1). In particular, the samples named TPU2 and TPU3 have a higher Young's modulus, which can be ascribed to the denser outer layer (concerning the core) of each foamed bead composing the sintered cylindrical sample. The Young's modulus of TPU3 is higher than the modulus of TPU2 due to the relatively thicker denser layer, marking a 30% increase concerning the uniform sample. Lastly, TPU4 has a slightly lower Young's modulus compared to the uniform sample (TPU1) because, in this case, the outer layer of each foamed bead is less dense than the core. The values of the Young's Modulus of both TPU and PS foamed samples are listed in Table 2.

TABLE 2 Young's modulus of the foamed PS samples

Sample	Young's modulus [MPa]	Variation with respect to uniform [%]	SD
TPU1	1.01	-	0.103
TPU2	1.12	+11%	0.188
TPU3	1.32	+31%	0.151
TPU4	0.98	−3%	0.112
PS1	0.95	-	0.029
PS2	1.06	+12	0.062
PS3	0.126	-	0.045
PS4	0.143	+13	0.101

These results confirm, both for the case of TPU and PS that mechanical properties in compression mode can be improved with the use of graded foamed beads. A new designing approach can be now foreseen to boost the development of advanced structures based on foams characterized by nonuniform spatial distribution of density and morphology.

4 | CONCLUSIONS

Commercial grade beads of PS and TPU were foamed using the novel graded foaming technology. The beads were foamed in molds where foaming and concurrent sinterization was achieved. The cellular structure design approach aimed to strengthen the interbeads regions in sintered foamed beads by manipulating the density and porosity distribution locally in each bead and the resulting mechanical properties accordingly. Use of molds allowed obtaining foams with the same average densities of 100 and 50 kg/m^3 for the PS and 100 kg/m^3 for TPU for the different samples characterized by uniform and graded morphologies for proper comparison. It was observed that Young's modulus of the foams formed by beads with a denser outer layer was higher concerning the uniform-reference-ones. A + 30% was observed with TPU and + 13% with PS. These results can be considered outstanding given the strong dependence of the foam Young's modulus on density with little chance for manipulation by other foam features.

DATA AVAILABILITY STATEMENT

No. Research data are not shared.

ORCID

Ernesto Di Maio https://orcid.org/0000-0002-3276-174X

REFERENCES

[1] U. G. K. Wegst, H. Bai, E. Saiz, A. P. Tomsia, R. O. Ritchie, *Nat. Mater.* **2014**, *14*, 23.
[2] H. Bai, Y. Chen, B. Delattre, A. P. Tomsia, R. O. Ritchie, *Sci. Adv.* **2015**, *1*, 107.
[3] A. H. Brothers, D. C. Dunand, *Adv. Eng. Mater.* **2006**, *8*, 805.
[4] N. Movahedi, G. E. Murch, I. V. Belova, T. Fiedler, *Mater. Des.* **2019**, *168*, 107652.
[5] Y. Hangai, K. Takahashi, T. Utsunomiya, S. Kitahara, O. Kuwazuru, N. Yoshikawa, *Mater. Sci. Eng. A.* **2012**, *534*, 716.
[6] J. Zeschky, T. Höfner, C. Arnold, R. Weißmann, D. Bahloul-Hourlier, M. Scheffler, P. Greil, *Acta Mater.* **2005**, *53*, 927.
[7] P. Colombo, J. R. Hellmann, *Mater. Res. Innov.* **2002**, *6*, 260.
[8] M. Trofa, E. Di Maio, P. L. Maffettone, *Chem. Eng. J.* **2019**, *362*, 812.
[9] J. Yu, L. Song, F. Chen, P. Fan, L. Sun, M. Zhong, J. Yang, *Mater. Today Commun.* **2016**, *9*, 1.
[10] L. Cui, S. Kiernan, M. D. Gilchrist, *Mater. Sci. Eng. A.* **2009**, *507*, 215.
[11] H. Niknam, A. H. Akbarzadeh, D. Rodrigue, D. Therriault, *Mater. Des.* **2018**, *148*, 188.
[12] J. T. Beals, M. S. Thompson, *J. Mater. Sci.* **1997**, *32*, 3595.
[13] I. Maskery, N. T. Aboulkhair, A.O. Aremu, C.J. Tuck, I. A. Ashcroft, R. D. Wildman, *Mater. Sci. Eng. A.* **2016**, *670*, 264.
[14] N. Gupta, W. Ricci, *Mater. Sci. Eng. A.* **2006**, *427*, 331.
[15] H. B. Zeng, S. Pattofatto, H. Zhao, Y. Girard, V. Fascio, *Int. J. Mech. Sci.* **2010**, *52*, 680.
[16] B. Koohbor, A. Kidane, *Mater. Des.* **2016**, *102*, 151.
[17] K. Z. Uddin, G. Youssef, M. Trkov, H. Seyyedhosseinzadeh, B. Koohbor, *J. Biomech.* **2020**, *109*, 109950.
[18] O. Polit, C. Anant, B. Anirudh, M. Ganapathi, *Compos. B Eng.* **2019**, *166*, 310.
[19] M. Kazemi, *Structures*. **2021**, *29*, 383.
[20] L. J. Gibson, M. F. Ashby, *Cellular Solids: Structure and Properties*, 2nd ed., Cambridge University Press, Cambridge **2014**.
[21] L. Di Landro, G. Sala, D. Olivieri, *Polym. Test.* **2002**, *21*, 217.
[22] E. Di Maio, S. Iannace, G. Mensitieri, *Foaming with Supercritical Fluids*, Elsevier Amsterdam, Netherlands **2021**.
[23] T. Standau, S. Goettermann, S. Weinmann, C. Bonten, V. Altstädt, *J. Cell. Plast.* **2016**, *53*, 481.

[24] C. Ge, Q. Ren, S. Wang, W. Zheng, W. Zhai, C. B. Park, *Chem. Eng. Sci.* **2017**, *174*, 337.
[25] M. Rubinstein, S. P. Obukhov, *Phys. Rev. Lett.* **1993**, *71*, 1856.
[26] S. Gupta, X. Yuan, T. C. Mike Chung, M. Cakmak, R. A. Weiss, *Polymer*. **2016**, *107*, 223.
[27] S. Roux, F. Hild, P. Viot, D. Bernard, *Compos. Part A Appl. Sci. Manuf.* **2008**, *39*, 1253.
[28] T. M. J. Gebhart, D. Jehnichen, R. Koschichow, M. Müller, M. Göbel, V. Geske, M. Stegelmann, M. Gude, *Int. J. Eng. Sci.* **2019**, *145*, 103168.
[29] A. S. S. Singaravelu, J. J. Williams, J. Ruppert, M. Henderson, C. Holmes, N. Chawla, *J. Mater. Sci.* **2020**, *56*, 5082.
[30] C. Marrazzo, E. Di Maio, S. Iannace, *J. Cell. Plast.* **2007**, *43*, 123.
[31] C. Zhou, P. Wang, W. Li, *Compos. Part B Eng.* **2011**, *42*, 318.

How to cite this article: F. Errichiello, A. Cammarano, E. Di Maio, L. Nicolais, *J. Appl. Polym. Sci.* **2021**, e52052. https://doi.org/10.1002/app.52052

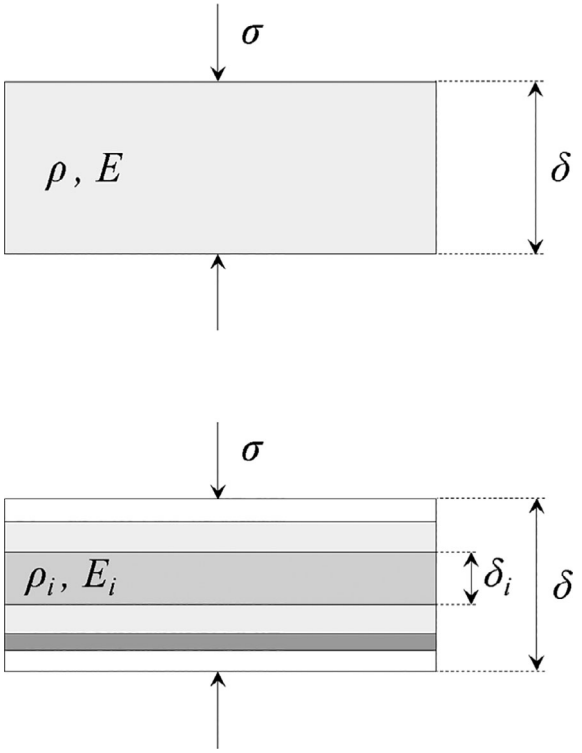

FIGURE A1 Scheme of the uniform and graded foam with density gradient parallel to compression load

APPENDIX A.

Consider a slab with thickness δ of a foam with uniform density ρ, subjected to a compressive load corresponding to a stress, σ (top scheme in Figure A1). By assuming, for simplicity, a typical dependence of the Young's modulus with the density (L. J. Gibson, M.F. Ashby, *Cellular solids: Structure and properties, Second edition*, Cambridge University Press, 2014, ISBN: 9781139878326).

$$\frac{E}{E_p} = \left(\frac{\rho}{\rho_P}\right)^2, \tag{A1}$$

where E_p and ρ_p are the Young's modulus and density of the neat, unfoamed polymer. A graded foam can be schematized by a finite number of foam layers, each characterized by the thickness δ_i and density ρ_i. For a proper comparison, the assumption that $\sum\delta_i = \delta$ and $\sum\delta_i\rho_i = \delta\rho$ was applied. In other words, for a proper comparison of a standard uniform foam and a layered one, the two samples have the same average density. This means that the sum of the average density of each layer of the graded foam matches the average density of the uniform equivalent foam.

When loaded in compression in the direction normal to layering (iso-stress mode) each layer is subjected to a deformation, ε_i:

$$\varepsilon_i \equiv \frac{\Delta\delta_i}{\delta_i} = \frac{\sigma}{E_i}, \tag{A2}$$

The deformation of the graded foam, $\overline{\varepsilon}$, is given by the weighted sum of the ith deformations:

$$\overline{\varepsilon} = \frac{\sum\Delta\delta_i}{\delta} = \frac{\sum\varepsilon_i\delta_i}{\delta}. \tag{A3}$$

Finally, the ratio between the Young's modulus of the graded foam, $\overline{E}$, and the one of the uniform foam, E, with same average density is given by:

$$\frac{\overline{E}}{E} = \frac{\varepsilon}{\overline{\varepsilon}} = \frac{\Delta\delta}{\sum\varepsilon_i\delta_i} = \frac{\frac{\delta}{E}}{\sum\frac{\delta_i}{E_i}}, \tag{A4}$$

which, by assuming valid Equation (A1) reads:

$$\frac{\overline{E}}{E} = \frac{\frac{\delta}{\rho^2}}{\sum\frac{\delta_i}{\rho_i^2}} = \frac{(\sum\delta_i)^3}{(\sum\delta_i\rho_i)^2}\frac{1}{\sum\frac{\delta_i}{\rho_i^2}}, \tag{A5}$$

which is always less than 1.

APPENDIX B.

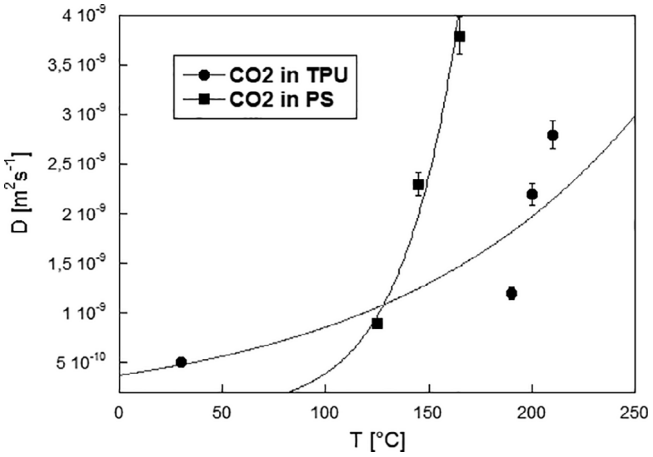

References

- H. Azimi, D. Jahani, *J. Supercrit. Fluids*, https://doi.org/10.1016/j.supflu.2018.05.010.
- R. Li, J. H. Lee, C. Wang, L. H. Mark, C. B. Park, *J. Supercrit. Fluids*, https://doi.org/10.1016/j.supflu.2019.104623.
- S. Ito, K. Matsunaga, M. Tajima, Y. Yoshida, *J. Appl. Polym. Sci*., https://doi.org/10.1002/app.26854.